PHYSICAL REVIEW D VOLUME 35, NUMBER 11 1 JUNE 1987

Baryon self-energies due to pion-quark coupling

M. Brack
Institute of Theoretical Physics, University of Regensburg, D-8400 Regensburg, Federal Republic of Germany

R. K. Bhaduri
Physics Department, McMaster University, Hamilton, Ontario, Canada, L8S 4M1

(Received 1 December 1986)

Pionic self-energy contributions to the nucleon and Δ are calculated perturbatively in the nonrelativistic constituent-quark model. The intermediate states are not restricted to the ground states of N and Δ. The difference in the self-energies of nucleon and Δ ground states converges satisfactorily, and may give rise to appreciable splitting if the hyperfine splitting from gluon exchange is less than 200 MeV. The results are very sensitive to the assumed axial size of the nucleon. For an axial radius of about 0.6 fm, the pionic self-energy contribution to the N-Δ splitting is approximately the same as found from the one-pion-exchange potential model. The difference in the pionic self-energies of the odd-parity excited states and the ground state is found to converge too slowly to make any definite statements.

I. INTRODUCTION

The aim of this paper is to examine the pionic self-energies of nucleon and Δ states in a nonrelativistic constituent-quark model, and their effect on spectroscopy. In the MIT bag model,[1] as well as most nonrelativistic quark models,[2,3] the baryon spectrum is generated from a phenomenological confinement of the quarks, and a quark-gluon interaction. In particular, the Δ-N mass difference in the ground state arises from the one-gluon-exchange mechanism.[4] Considerations of chiral symmetry prompted the introduction of pions as elementary fields coupled to quarks.[5] In the cloudy-bag model,[6,7] the pion-quark interaction is linearized, and the difference in self-energy in the ground states of N and Δ is calculated by restricting the intermediate states to the ground states of N and Δ. Pions have also been introduced in nonrelativistic constituent-quark models.[8–10] The spectroscopy has been studied in Ref. 10. In Refs. 9 and 10, however, the pionic effects are calculated from the one-pion-exchange potential between the nonstrange quarks. The aim here is to calculate such effects consistently from the pionic contribution to the baryon self-energies, in the ground and low-lying odd-parity excited state.

Complications in the self-energy problem due to pions arise when the intermediate states of the nucleon (or Δ) are allowed to take all possible configurations. It was shown that with a sharp bag surface (such as the MIT bag) the contribution of the pion self-energy to the nucleon diverges,[11] even if a pionic form factor is introduced. Various remedies to this problem have been proposed, including a smeared bag surface.[12] The self-energy of a nucleon (or Δ) due to pion coupling has also been calculated in the nonrelativistic constituent-quark model.[8] It has been shown[13] recently that in the oscillator model the self-energy of the nucleon does not diverge if a pionic form factor is introduced. It is also claimed[13] that the pionic contribution to the N-Δ mass difference, calculated perturbatively, is negligible once the spin dependence of the quark-gluon interaction is taken properly into account. This is disturbing, since all models where pionic effects contribute substantially[10] to N-Δ mass splittings would then be suspect. Much of the effort in the present paper goes into a detailed study of the N-Δ ground-state splitting due to pionic self-energy. We show that the results are extremely sensitive to the assumed radius of the nucleon. This is not the electromagnetic radius, but is for the axial charge. With an appropriate pionic form factor, we find that an appreciable part of the N-Δ mass difference may arise from pionic self-energy effects. Nevertheless, it is partly true that the use of just the one-pion-exchange potential overestimates such effects.[13] We also find that it is misleading, in the self-energy calculations, to exclude all but the ground-state configurations of the N and Δ.

In this paper the self-energy calculations are performed in second-order perturbation theory using properly symmetrized harmonic-oscillator wave functions, and including all intermediate states from oscillator quantum number $N=0$ to $N=3$. Two simple, but different patterns of the excitation spectrum are taken to show that the final result is not sensitive to the details of the spectrum. With a simple harmonic spectrum, we show analytically that the *difference* between the nucleon and Δ self-energies is convergent even without a pionic form factor, although the individual contributions diverge. We also calculate the self-energies of the odd parity $N=1$ states of N and Δ. However, in this case, the convergence is found to be very poor, and we are unable to give any definite results.

In Sec. II we describe the model and the assumption made in the calculation. The results are presented and discussed in Sec. III. Appendixes A and B contain, in addition to the general formula for the matrix element of the pion-quark interaction between appropriate states, a list of properly symmetrized oscillator states of N and Δ up to the oscillator shell $N=3$. The latter are listed mainly for convenience and the completeness of notation.

II. THE MODEL

The self-energy of the nucleon due to the pionic interaction is calculated in second-order perturbation theory. We write the total Hamiltonian as

$$H=H_0+H_\pi+h_{qq\pi}\ , \tag{1}$$

where the part H_0 consists of the three constituent quarks moving in an appropriate confinement potential, and interacting with each other by gluon exchange. The next term is the free pion Hamiltonian. Following the philosophy of Ref. 13, we assume that the energy spectrum generated by H_0 is known, and its eigenstates can be well approximated by harmonic-oscillator wave functions. Using Jacobi coordinates, the center-of-mass variable is eliminated easily. Note that H_0 already yields a mass difference between the $T=\frac{3}{2}$ and $T=\frac{1}{2}$ ground states, and we denote this difference by δ_g. Soon we shall describe the assumed spectrum of H_0 in two separate scenarios. The interaction Hamiltonian $h_{qq\pi}$ is taken to be

$$h_{qq\pi}=\frac{g_{qq\pi}}{2m_q}\sum_{i=1}^{3}\sum_{\alpha}\tau_\alpha(i)\sigma(i)\cdot\nabla\phi_\alpha(\mathbf{r}_i)\ , \tag{2}$$

where the nonrelativistic limit of pseudoscalar coupling has been taken. The pseudovector coupling yields the same form, with the factor $g_{qq\pi}/2m_q$ replaced by $\sqrt{4\pi}f_{qq\pi}/m_\pi$. Here m_q is the mass of the constituent quark, and m_π that of the pion. The sum i goes over the three quarks, and α denotes the isospin index. The pseudoscalar field ϕ_α as usual creates or destroys a pion:

$$\phi_\alpha=\sum_k\frac{1}{\sqrt{2\omega_k}}(a_{k,\alpha}e^{i\mathbf{k}\cdot\mathbf{r}}+a^\dagger_{k,\alpha}e^{-i\mathbf{k}\cdot\mathbf{r}})\ . \tag{3}$$

We use the formalism of old-fashioned perturbation theory, where even virtual pions are on the mass shell, i.e., $\omega_k=(k^2+m_\pi^2)^{1/2}$, but the energy is not conserved at each vertex. Furthermore, for *virtual* pions, a pion-nucleon axial form factor is inserted at each vertex. Guided by the vector-dominance model, we take the form

$$F_\pi(\mathbf{k}^2)=\frac{1}{1+\mathbf{k}^2/\Lambda_\pi^2}\ , \tag{4}$$

where $\Lambda_\pi=1275$ MeV corresponding to the mass of the meson a_1 (1275). Note that the axial radius of the nucleon is known from neutrino scattering experiments:[14]

$$\langle r_a^2\rangle^{1/2}=0.68\pm0.02\ . \tag{5}$$

To write down the expression for the self-energy contribution Σ_π, we assume that the spectrum of H_0 in Eq. (1) is known, and is given by

$$H_0\,|\,\psi_B\rangle=E_B\,|\,\psi_B\rangle\ , \tag{6}$$

where B stands for N, Δ, or the excited states of these, properly symmetrized and with the appropriate quantum numbers. The gluonic hyperfine splitting is denoted by

$$\delta_g=E_\Delta-E_N\ , \tag{7}$$

and is only a certain fraction of the experimental mass difference $(M_\Delta-M_N)$. In this perturbative scheme, the self-energy of the Δ, for example, due to the pionic interaction is

$$\Sigma_\pi(\Delta)=\frac{1}{(2\pi)^3}\int d^3k\sum_B\frac{\langle\psi_B,\mathbf{k}\,|\,h_{qq\pi}\,|\,\psi_\Delta\rangle\,|^2}{E_\Delta-(E_B+\omega_k)}\ , \tag{8}$$

where the sum B goes over all states of Eq. (6). This corresponds to Fig. 1. Note that in the above sum when $B=N$, the nucleon ground state, there is a pole in the integral, and Σ_π is complex. The width of the Δ due to real pion decay is proportional to the imaginary part[15] of this Σ_π. In such a calculation, since only real pions are emitted, $F_\pi=1$, and moreover $(E_\Delta-E_N)$ in the denominator of Eq. (8) should be replaced by the actual mass difference $(M_\Delta-M_N)$. If recoil of the nucleon is neglected, one gets the simple expression in the oscillator model:

$$\Gamma_\pi(\Delta\to N\pi)=\tfrac{4}{3}k^3\frac{\alpha_\pi}{m_q^2}e^{-k^2/3\alpha_0^2}\ . \tag{9}$$

Here $\alpha_0=\sqrt{m_q\Omega}$, Ω being the oscillator spacing, and $\alpha_\pi=g_{qq\pi}^2/4\pi$. Note that the coefficient α_π/m_q^2 is also written as $4f_{qq\pi}^2/m_\pi^2$. The pion momentum k is determined by energy (and momentum) conservation $k=227$ MeV/c. Inclusion of recoil effects alters Eq. (9) to[16]

$$\Gamma_\pi(\Delta\to N\pi)=\tfrac{4}{3}k^3\frac{\alpha_\pi}{m_q^2}\frac{E_N}{M_\Delta}e^{-k^2/3\alpha_0^2}\ , \tag{10}$$

with $E_N=(k^2+M_N^2)^{1/2}$. We shall come back to this problem presently.

When calculating the real part of $\Sigma_\pi(\Delta)$ from Eq. (8), one should multiply the integrand on the right by $F_\pi^2(k)$, since only virtual pions are involved. Consider the self-energy of a baryon i due to the process $(i\to B\pi\to i)$. The angular momentum algebra simplifies after one averages over the spin states of i and sums over all spin-isospin states of B. Writing

$$\overline{|\langle\psi_B,\mathbf{k}\,|\,h_{qq\pi}\,|\,\psi_i\rangle\,|^2}=\frac{1}{2\omega_k}\overline{|\mathscr{M}_{Bi}\,|^2}\ ,$$

we get, taking the principal value of the integral in Eq. (8),

$$\Sigma_\pi(i)=-\frac{1}{4\pi^2}\sum_B P\int_0^\infty\frac{k^2\overline{|\mathscr{M}_{Bi}\,|^2}F_\pi^2(k)dk}{\omega_k[\omega_k-(E_B-E_i)]}\ , \tag{11}$$

where the quantity $\overline{|\mathscr{M}_{Bi}\,|^2}$ may be calculated using harmonic-oscillator wave functions. When the state i

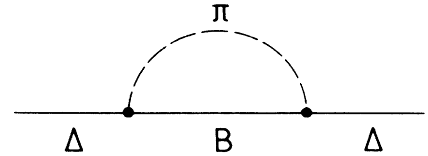

FIG. 1. Pionic self-energy contribution to the Δ mass, due to intermediate state B.

stands for the ground state N or Δ, we get

$$\overline{|\mathscr{M}_{Bi}|^2}=\eta_{Bi}\frac{\pi}{3}\frac{\alpha_\pi}{m_q^2}k^2\exp\left[-\frac{k^2}{3\alpha_0^2}\right]. \qquad (12)$$

Here η_{Bi} are dimensionless coefficients given in Eq. (B16) and Tables III and IV. The generalization of this formula for the excited states is also given in Appendix B. Restricting the sum over B to ground state only (which is *not* a good approximation in our model), we get

$$\Sigma_\pi(N)=-\frac{\alpha_\pi}{m_q^2}\frac{1}{12\pi}\int_0^\infty\frac{dk\,k^4}{\omega_k}F_\pi^2(k)\left[\frac{25}{\omega_k}+\frac{32}{\omega_k+\delta_g}\right]e^{-k^2/3\alpha_0^2}$$

and

$$\Sigma_\pi(\Delta)=-\frac{\alpha_\pi}{m_q^2}\frac{1}{12\pi}P\int_0^\infty\frac{dk\,k^4F_\pi^2(k)}{\omega_k}\left[\frac{25}{\omega_k}+\frac{8}{\omega_k-\delta_g}\right]e^{-k^2/3\alpha_0^2}. \qquad (13)$$

Care should be exercised in taking the principal value of the last integral in the second line of Eq. (13). These are standard equations which have been used before.[7] In this paper we also derive η_{Bi} for all the excited states up to oscillator quantum number $N=3$, and present the numerical results in the next section. These excited-state wave functions are tabulated for completeness in Appendix A.

From Eq. (13), we note that the $N=0$ contribution to the mass difference $\Sigma_\pi(\Delta)-\Sigma_\pi(N)$ arises entirely from $N\to\Delta+\pi$ or $\Delta\to N+\pi$ type of processes. It is common practice to fix the pion-quark coupling constant in the nonrelativistic models through the relation[16]

$$\frac{\alpha_\pi}{m_q^2}=\left[\frac{3}{5}\right]^2\frac{1}{M_N^2}\frac{g_{NN\pi}^2}{4\pi}, \qquad (14)$$

where from πN scattering we know $g_{NN\pi}^2/4\pi=14.4$. This yields $\alpha_\pi=0.64$ for $m_q=330$ MeV. Alternatively, the same constraint fixed the pseudovector pion-quark coupling constant

$$f_{qq\pi}^2=(\tfrac{3}{5})^2f_{NN\pi}^2 \text{ with } f_{NN\pi}^2=0.08. \qquad (15)$$

It is well known that this causes problems in the width of the Δ, $\Gamma_\pi(\Delta\to N\pi)$. From Eq. (9) if we take the oscillator spacing $\Omega=550$ MeV, $m_q=330$ MeV, and $\alpha_\pi=0.64$, we get $\Gamma_\pi(\Delta\to N\pi)\approx 83$ MeV, compared to the experimental value of 115 MeV. It is possible that higher-order diagrams in the calculation of Γ_π may resolve this discrepancy.[17] But in a calculation such as ours which is of first order in α_π, we prefer to choose an effective value that fits the width $\Gamma_\pi(\Delta\to N+\pi)$ with the naive formula (9), giving $\alpha_\pi=0.88$. This is equivalent to the choice[18] of

$$f_{N\Delta\pi}^2=0.32\approx 4f_{NN\pi}^2, \qquad (16)$$

rather than $f_{N\Delta\pi}^2=\frac{75}{25}f_{NN\pi}^2=0.23$. We choose the value (16) in the calculation of the self-energy difference $\Sigma_\pi(\Delta)-\Sigma_\pi(N)$, because, as seen from Eq. (13), it is only the $N\Delta\pi$ coupling that is relevant here. Moreover, the same value of the coupling constant α_π yields a better fit[16] to pionic widths of $N^*\to N+\pi$, etc., rather than the smaller value $\alpha_\pi=0.64$. We shall therefore use $\alpha_\pi=0.88$ for all transitions from the ground to excited states B.

To perform a calculation in which the excited-state transitions are included, the spectrum of the energies E_B appearing in Eq. (6) is to be specified. We choose two such models. In model A

$$H_0=\frac{1}{2m_q}(p_\rho^2+p_\lambda^2)+\tfrac{1}{2}m_q\Omega^2(\rho^2+\lambda^2)+h_s, \qquad (17)$$

where h_s is the hyperfine interaction between quarks due to the one-gluon-exchange potential. For simplicity, it is taken to be a zero-range two-body potential.[3] It is to be regarded as an effective interaction whose diagonal elements yield the appropriate hyperfine splitting for each state. The ground-state splitting, Eq. (7), then becomes

$$\delta_g=2\sqrt{2}\,\alpha_s\alpha_0^3/(3\sqrt{\pi}m_q^2), \qquad (18)$$

with α_s the effective quark-gluon coupling constant, and $\alpha_0=\sqrt{m_q\Omega}$. In summing over the intermediate states B in Fig. 1, all excitations to shells $N\geq 4$ are ignored. For simplifying the calculation, h_s is dropped in the $N=3$ shell.

Model A has the disadvantage that the excited states with $N=2$ and 3 are too high in energy compared to experiment. Following the prescription of Ref. 3, one may assume that the $N=2$ states are brought down near the $N=1$ states by a pattern shown in Fig. 2, which reflects the anharmonic components of the interaction. Such a spectrum (model B) of E_B's is shown in Fig. 2. Some of the $N=3$ odd-parity states are known experimentally at about 2 GeV, but most of them are not identified. Rather arbitrarily, the {56} $L=1^-N$ and Δ states are placed around this energy, while all the other $N=3$ states are put 300 MeV higher. The hyperfine splittings due to the gluonic part h_s for all states are the same as in model A.

III. RESULTS AND DISCUSSION

A. Ground-state N-Δ splitting

We first concentrate on the pionic contributions to the ground-state N-Δ splitting:

$$\delta_\pi=\Sigma_\pi(\Delta)-\Sigma_\pi(N). \qquad (19)$$

Let us discuss first the often-used approximation[6,19] of re-

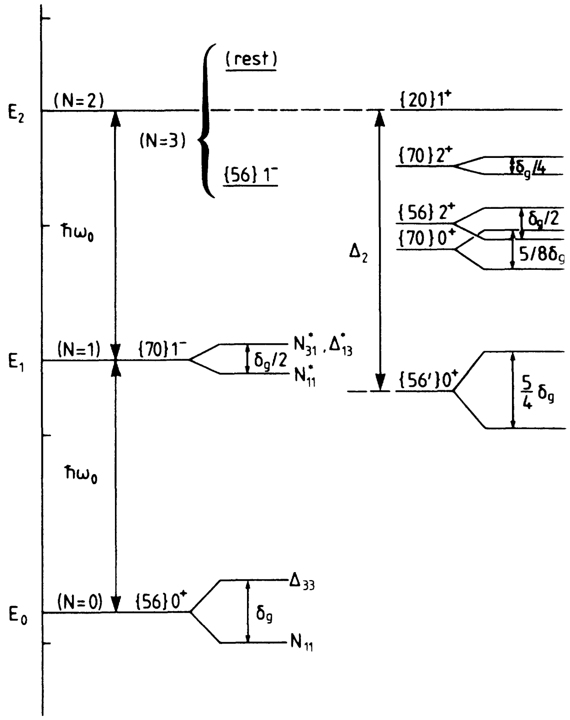

FIG. 2. Schematic harmonic-oscillator baryon spectrum with spacing $\hbar\omega_0$ ($=\Omega$ in the text), modified by gluonic hyperfine splitting (parameter δ_g) and, for $N=2$, anharmonic splittings (parameter Δ_2). Choice of parameters for "model B": $\Omega=550$ MeV, $\Delta_2=600$ MeV.

stricting the intermediate states to the ground states N and Δ. From Eq. (13) we then obtain ($N'=0$ denoting the contribution of this shell only)

$$\delta_\pi(N'=0)=\frac{\alpha_\pi}{m_q^2}\frac{1}{12\pi}\int_0^\infty dk\frac{k^4F_\pi^2(k)e^{-k^2/3\alpha^2}}{\omega_k}\times\left[\frac{32}{\omega_k+\delta_g}-\frac{8}{\omega_k-\delta_g}\right], \quad (20)$$

where the principal value of the last integral is taken. For the special case of $\delta_g=0$, this becomes

$$\delta_\pi^{(0)}(N'=0)=\frac{\alpha_\pi}{m_q^2}\frac{2}{\pi}\int_0^\infty dk\frac{k^4F_\pi^2(k)e^{-k^2/3\alpha^2}}{\omega_k^2}. \quad (21)$$

The superscript (0) in $\delta_\pi^{(0)}$ is to remind the reader that $\delta_g=0$ here. This expression is of some interest for comparison with the potential model.[10] In the latter, one simply takes the one-pion-exchange potential (OPEP) (including the δ-function part) between quarks, and calculates the splitting $\langle\psi_\Delta | V_{\rm OPEP} | \psi_\Delta\rangle - \langle\psi_N | V_{\rm OPEP} | \psi_N\rangle$. One can evaluate these expectation values directly in momentum space:

$$\langle\psi_N | V_{\rm OPEP} | \psi_N\rangle = \int \langle\psi_N | \mathbf{k}\rangle\langle\mathbf{k} | V_{\rm OPEP} | \mathbf{k}'\rangle \times\langle\mathbf{k}' | \psi_N\rangle d^3k\, d^3k' , \quad (22)$$

where, in the static approximation,[20]

$$\langle\mathbf{k} | V_{\rm OPEP} | \mathbf{k}'\rangle = -\frac{\alpha_\pi}{4m_q^2}\frac{4\pi}{(2\pi)^3}(\tau_1\cdot\tau_2)\frac{(\sigma_1\cdot\mathbf{q})(\sigma_2\cdot\mathbf{q})}{\omega_q^2} \quad (23)$$

with $\mathbf{q}=\mathbf{k}'-\mathbf{k}$. By taking the harmonic-oscillator ground-state wave functions in momentum space in Eq. (22), it is straightforward to show that

$$\delta_\pi({\rm OPEP})=\frac{\alpha_\pi}{m_q^2}\frac{2}{\pi}\int_0^\infty dq\frac{q^4F_\pi^2(q)e^{-q^2/2\alpha^2}}{\omega_q^2} . \quad (24)$$

Note the difference with Eq. (21)—the exponent is $\exp(-q^2/2\alpha^2)$ rather than $\exp(-q^2/3\alpha^2)$, but otherwise the expressions are identical. This shows that the most naive self-energy calculation for the splitting $\delta_\pi^{(0)}$, using Eq. (21), overestimates the result compared to the potential model approach of Eq. (24), if the same parameters are used. This is in contrast with Ref. 13, where the two were identical because of a spurious center-of-mass contribution in the self-energy part.

It was pointed out in Ref. 13 that for $\delta_g>0$, one gets $\delta_\pi<\delta_\pi^{(0)}$, as is clear from Eqs. (20) and (21). It is also correct[13] that if δ_g is taken close to the N-Δ experimental splitting, then δ_π is small. The actual numbers depend rather sensitively on the parameters of the model, in particular on the axial radius $\langle r_A{}^2\rangle^{1/2}$ that is determined by the choice of Λ_π. (This will be demonstrated in Fig. 3.)

Till now we have been discussing the approximation where the intermediate states B in the self-energy diagram (Fig. 1) can only be N and Δ, corresponding to the $N=0$ shell of the oscillator model. Actually the contribution of the intermediate excited states is far from negligible. In particular, the $N=1$ odd-parity excited states lower the Δ relative to the N, and as much as one-half to one-third of the ground-state contribution [Eq. (20)] is canceled by this. This may be seen from Table I, where the contributions of the intermediate states B (with oscillator quantum numbers $N'=0,1,2$, etc.) to the ground-state splitting δ_π

TABLE I. Pionic contributions to the ground-state N-Δ splitting δ_π (in MeV) from intermediate states with oscillator quantum number N'. Parameters: $\Omega=550$ MeV, $m_q=330$ MeV, $\Lambda_\pi=1275$ MeV, $\alpha_\pi=0.88$.

	Model A		Model B	
N'	$\delta_g=0$	$\delta_g=140$ MeV	$\delta_g=0$	$\delta_g=140$ MeV
0	445.1	286.7	445.1	286.8
1	−149.9	−165.3	−149.9	−165.4
2	56.0	40.0	73.4	51.3
3	−21.7	−29.9	−21.6	−33.9
4	8.6			
5	−3.4			
6	1.5			
7	−0.6			
8	0.26			
9	−0.10			
Sum	335.8	131.8	347.1	138.8

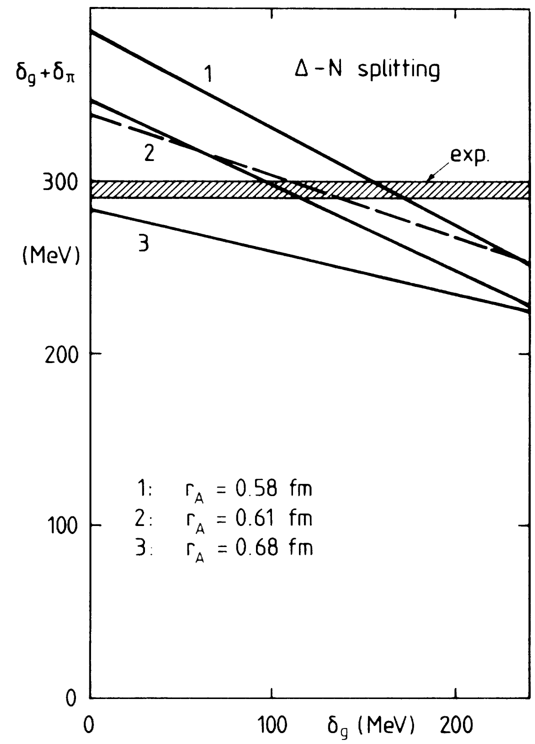

FIG. 3. Total ground-state Δ-N splitting $\delta_\pi+\delta_g$ vs gluonic hyperfine splitting δ_g. The three solid lines correspond to the axial radii r_A given on the figure. Spectrum of model B (see Fig. 2). Parameters: $m_q=330$ MeV, $\alpha_\pi=0.88$, $\Lambda_\pi=1.275$ GeV (1 + 2), $\Lambda_\pi=0.97$ GeV (3); $\Omega=550$ MeV and $\Delta_2=600$ MeV (2 + 3); $\Omega=600$ MeV and $\Delta_2=680$ MeV (1). Dashed line: same parameters as solid line No. 2, but including recoil of the intermediate baryon (see text); $\alpha_\pi=1.13$.

are shown explicitly.

We first discuss in Table I the more tractable model A of equidistant excited states, and take the specially simple case with $\delta_g=0$. A pattern clearly emerges from the numbers in column A: the contributions to δ_π from the even shell ($N'=0,2,4$) are positive, while those from the odd states are negative. From the tableaux of matrices W_{Bi} in Table III and Eqs. (B15) and (B16) it is clear that the spatially symmetric intermediate states [corresponding to the {56} representation in SU(6)] increase δ_π, while the {70} states reduce it. From the latter, for example, the Δ gets exactly twice the contribution to its (negative) self-energy than the nucleon, thus reducing δ_π. Note that this effect, leading to contributions from successive shells with alternating signs, is arising purely from the overall symmetrization of the states B, and the SU(6) spin-isospin matrix elements through the coefficients W_{Bi} which do not depend on the other details of the model (e.g., this would be the same as in the cloudy-bag model).

For the particularly simple case with $\delta_g=0$, the appropriate coefficients η_{Bi} of Eq. (12) may be collected from Eq. (B16) and Tables III and IV to yield

$$\delta_\pi^{(0)}=\frac{\alpha_\pi}{m_q^2}\frac{2}{\pi}\int_0^\infty dk\frac{k^4F_\pi^2(k)}{\omega_k}e^{-k^2/3\alpha_0^2}I(k) \qquad (25)$$

with

$$I(k)=\sum_{N'=0}^{\infty}\frac{(-1)^{N'}}{N'!}\left[\frac{1}{6}\frac{k^2}{\alpha_0^2}\right]^{N'}\frac{1}{\omega_k+N'\Omega} . \qquad (26)$$

Equation (25) is a generalization of Eq. (21). The numerical contribution of each shell to δ_π is tabulated in the second column of Table I. These converge reasonably fast, with successive terms alternating in sign and decreasing in magnitude. For example, if the sum is truncated at $N'=3$, about 6 MeV is missed in δ_π—a result good to 2%. The convergence can be seen analytically also, by noticing that

$$\begin{aligned}I(k)&=\sum_{N'=0}^{\infty}\frac{(-)^{N'}}{N'!}t^{N'}\frac{1}{\omega_k+N'\Omega}\\&=\int_0^\infty dx\,\exp(-\omega_k x-te^{-\Omega x})\end{aligned} \qquad (27)$$

with $t=\frac{1}{6}k^2/\alpha_0^2$. Taking the limits $\Omega\to 0$ and $\Omega\to\infty$, we can find both an upper and a lower bound for $I(k)$:

$$\frac{e^{-t}}{\omega_k}\le I(k)\le\frac{1}{\omega_k} .$$

(The left-hand equality holds only for $\Omega=0$, the right-hand one only for $\Omega=\infty$.) It then follows from Eqs. (21), (24), and (25) that, for finite Ω,

$$\delta_\pi(\text{OPEP})<\delta_\pi^{(0)}<\delta_\pi^{(0)}(N'=0) . \qquad (28)$$

Since $\delta_\pi^{(0)}(N'=0)$ Eq. (21) is finite, we have proved the convergence of $\delta_\pi^{(0)}$, even for $F_\pi^2(k)=1$. Note, however, that if $F_\pi^2(k)=1$, but $\delta_g\neq 0$, then δ_π diverges.

It does not seem possible to write a single series as in Eq. (25) for the more realistic case of $\delta_g\neq 0$. From Table I it will be seen that with $\delta_g=0.14$ GeV, there is a substantial quenching of the positive contributions from the even-parity states ($N'=0,2$) and an enhancement from the odd states. The self-energy δ_π is therefore cut down substantially when $\delta_g=140$ MeV, but $(\delta_g+\delta_\pi)$ is close to the experimental mass difference $(M_\Delta-M_N)$. Moreover, although the spectrum of model B is very different from that of model A, the self-energy difference δ_π is about the same in either mode.

We found numerically that δ_π decreases linearly with increasing δ_g up to $\delta_g\simeq 250$ MeV. In Fig. 4 we show δ_π as a function of δ_g, obtained with the spectrum of Model B for a set of parameters corresponding to $\langle r_A^2\rangle^{1/2}=0.61$ fm as in Table I ($\Omega=550$ MeV, $m_q=330$ MeV, $\Lambda_\pi=1275$ MeV). It is seen that for $\delta_g\simeq 230$ MeV, δ_π becomes zero and, for larger δ_g, even negative. This can only happen when the intermediate states with $N'>0$ are included. The dashed curve in Fig. 4 shows the approximation $\delta_\pi(N'=0)$ which is easily seen also from Eq. (20) to stay positive and to vanish like δ_g^{-1} for large δ_g. With a choice of $\delta_g\simeq 100$ MeV, the pionic contribution δ_π is about 200 MeV, so that the sum of δ_g and δ_π gives the experimental N-Δ splitting.

However, these results are particularly sensitive to the axial radius of the nucleon. This is demonstrated in Fig. 3, where we show the total N-Δ splitting, i.e., the sum

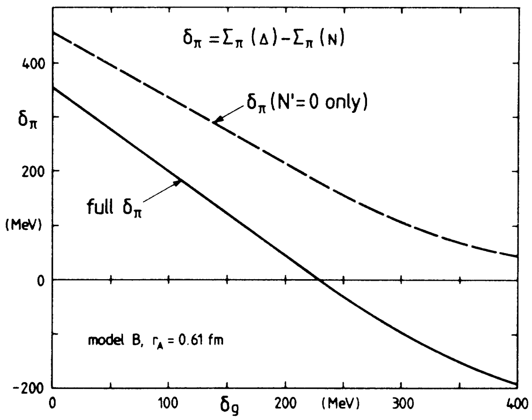

FIG. 4. Pionic contribution δ_π to the ground-state N-Δ splitting δ_g. Dashed line: using intermediate states with $N'=0$ (i.e., N and Δ) only. Solid line: including intermediate states up to $N'=3$. Parameters as in Fig. 2 and Table I.

$(\delta_g + \delta_\pi)$, plotted versus δ_g for model B. Different parameter sets have been used corresponding to the axial radii $r_A = \langle r_A{}^2 \rangle^{1/2}$ indicated on the figure. With the choice of $\Omega = 550$ MeV, $m_q = 330$ MeV, one needs $\Lambda_\pi = 970$ MeV to reproduce the experimental axial radius $\langle r_A{}^2 \rangle^{1/2} = 0.68$ fm. Even when α_π is taken to be 0.88, $(\delta_g + \delta_\pi)$ is found to be short of the experimental value, though not by much. For $\Lambda_\pi = 1275$ MeV, $\langle r_A{}^2 \rangle^{1/2} = 0.61$ fm, as we have seen above, about two-thirds of the N-Δ splitting arises from the pions. With an even smaller radius of $\langle r_A{}^2 \rangle^{1/2} = 0.58$ fm, the self-consistent solution yields about half the splitting coming from the pions. We emphasize that these results should not be taken too literally, since the model is so crude. But it is clear from these discussions that if the gluonic hyperfine splitting δ_g is assumed not to exceed 200 MeV, the pionic contribution to the N-Δ mass difference may be substantial. For $\delta_g > 200$ MeV, we are not able to find a self-consistent solution with $\delta_\pi + \delta_g \simeq 300$ MeV for any reasonable radius r_A. This is at variance with the results of the cloudy-bag model,[7,21] where the intermediate states with $N' > 0$ were ignored.

In the calculations so far, we have neglected the effect of recoil of the baryon as the virtual pion is emitted. This can be taken into account by replacing $(E_B - E_i)$ in the denominator of Eq. (11) by $[(E_B{}^2 + k^2)^{1/2} - E_i]$. To be consistent, however, one should then choose α_π by fitting the width $\Gamma_\pi(\Delta \to N\pi)$ from Eq. (10), rather than Eq. (11). Such a procedure requires $\alpha_\pi = 1.13$ rather than 0.88, the latter value being for the static approximation. In Fig. 3 we also show the result of such a calculation in which recoil has been taken into account with $\alpha_\pi = 1.13$. If the radius r_A is not changed, the result differs little from the static calculation.

We have remarked before that in some earlier calculations,[10] the one-pion-exchange potential has been used, together with the form factor squared $F_\pi{}^2$ to estimate pionic effects in the spectrum. The explicit form of the form-factor modified potential is given in Ref. 10, and is irrelevant here. Its contribution to δ_π is given simply by Eq. (24). It is of interest to make some numerical comparison of this with the more difficult self-energy approach. For such a comparison, we evaluate Eq. (24) with $F_\pi(k)$ given by Eq. (4). Taking the same parameters as in the self-energy calculation, i.e., $\hbar\Omega = 550$ MeV, $\Lambda_\pi = 1275$ MeV, and $m_q = 330$ MeV, we find that

$$\delta_\pi(\text{OPEP}) = 312\alpha_\pi \text{ MeV} \quad (\Lambda_\pi = 1275 \text{ MeV}) . \tag{29}$$

When one is using the OPEP, it may be more reasonable to use Eq. (14) to fix α_π, which yields $\alpha_\pi = 0.64$. Equation (24) then gives $\delta_\pi(\text{OPEP}) = 200$ MeV, so the other 100 MeV must come from gluonic hyperfine splitting δ_g. Note that in the potential approach, the quantity δ_π(OPEP) is independent of δ_g, unlike the self-energy problem. Nonetheless, a glance at Fig. 4 will show that the self-energy calculation with the same parameters (but with $\alpha_\pi = 0.88$) yields the same result $\delta_\pi \approx 200$ MeV, $\delta_g \approx 100$ MeV. This agreement may be fortuitous, since both results depend sensitively on the choice of Λ_π. If, however, we restrict Λ_π in the range 1000–1300 MeV, the OPEP model results with $\alpha_\pi = 0.64$ are not too different from the self-energy calculation (including excited intermediate states, and with $\alpha_\pi = 0.88$).

B. Self-energy of the odd-parity excited states

For spectroscopy, it is important to find out about the state dependence of the pionic self-energy. When using the OPEP model for the pionic effect, the potential consists of a δ-function piece and the usual Yukawa form,[10] if $F_\pi = 1$. The dominant contribution to the matrix elements arises from the δ-function part. From this, a little consideration shows that the pionic matrix element is nearly halved in the odd-parity $N=1$ shell compared to the $N=0$ ground state in the OPEP model. For example, we know that in the ground state, the nucleon is depressed five times more than the Δ by the OPEP. If the Δ is depressed by x, then the spin-isospin-weighted shift in the $N=0$ state is $\frac{1}{20}(4\times 5x + 16\times x) = 1.8x$. From Eq. (28), it then follows that the weighted shift in the $N=0$ state due to OPEP is $-140\alpha_\pi$ (in MeV) for $\Lambda_\pi = 1275$ MeV. A similar consideration in the odd-parity $N=1$ shell gives a mean shift of $0.9x$. It follows that, for the mean,

$$\langle V_{\text{OPEP}} \rangle_{N=1} - \langle V_{\text{OPEP}} \rangle_{N=0} = 70\alpha_\pi \text{ MeV} , \tag{30}$$

which is about 45 MeV for $\alpha_\pi = 0.64$. In order to compare this result with the corresponding self-energy calculation, we attempted to calculate Σ_π for the nucleon and Δ $N=1$ odd-parity excited states using the general Eq. (11). Again only intermediate states up to $N'=3$ were considered. In Table II the spin-isospin-weighted pionic self-energy contribution to the $N=0$ and $N=1$ states are shown, arising from the different shells. The quantity corresponding to Eq. (30), denoted by

$$\Delta_\pi = [\bar{\Sigma}_\pi(N=1) - \bar{\Sigma}_\pi(N=0)] \tag{31}$$

is also shown in Table II, where the bar on Σ_π denotes the spin-isospin average. In computing $\bar{\Sigma}_\pi(N=1)$, since the space is truncated at $N'=3$, the maximum $\Delta N = N' - N = 2$. It is therefore reasonable to compute

TABLE II. Contributions (in MeV) to the spin-isospin-averaged pionic self-energies $\bar{\Sigma}_\pi$ of the ground states ($N=0$) and the $N=1$ (odd-parity) states due to intermediate states N'. Parameters as in Table I; Model B. See text for value of α_π. The last two columns show $\Delta_\pi=\bar{\Sigma}_\pi(N=1)-\bar{\Sigma}_\pi(N=0)$ and $\delta_\pi(N=1)=\Sigma_\pi(\Delta^*_{13})-\Sigma_\pi(N^*_{11})$. $\delta_g=140$ MeV.

$\Delta N=N'-N$	$\bar{\Sigma}_\pi(N=0)$	$\bar{\Sigma}_\pi(N=1)$		Δ_π	$\delta_\pi(N=1)$	
0	-594.9		-324.4	270.5		67.1
$+1$	-276.8	-238.8	-636.1	-359.3	-32.3	-2.0
-1		-352.3			30.3	
$+2$	-325.1		-227.1	98.0		-36.7
Sum	-1196.8		-1187.6	9.2		28.4

$\bar{\Sigma}_\pi(N=0)$ also to the same approximation in Eq (31), taking only up to $N'=2$. In the calculation of these self-energies, we took $\alpha_\pi=0.64$ for transitions such as $N\to N+\pi$ or $\Delta\to\Delta+\pi$, but increased it to 0.88 for transitions $\Delta\to N+\pi$, $N^*\to N+\pi$, etc., due to the reasons discussed in Sec. II.

The quantity Δ_π [Eq. (31)] will be seen from Table II to be rather small, although the convergence of its contributions from the intermediate states is rather poor. With some optimism, we may conclude that Δ_π will probably be below 100 MeV in magnitude, so that no drastic modification of the main shell spacing Ω may be needed in conventional spectroscopy due to the pionic self-energy.

For completeness, we have also shown in the last column of Table II the contribution to the quantity

$$\begin{aligned}\delta_\pi(N=1)&=\Sigma_\pi(\Delta^*_{13})-\Sigma_\pi(N^*_{11})\\&=\Sigma_\pi(N^*_{31})-\Sigma_\pi(N^*_{11})\ ,\end{aligned}\tag{32}$$

which is the analog to δ_π Eq. (19), but in the odd-parity $N=1$ shell. (Note that the states N^*_{31} and Δ^*_{13} of the $\{70\}$ multiplet remain degenerate.) The convergence is again too poor to make any definitive statements. But, clearly, the splitting $\delta_\pi(N=1)$ is substantially smaller than δ_π [Eq (19)] in the ground state (see the last column of Table I, evaluated with the same parameters), in qualitative agreement with the OPEP result $\delta_\pi(N=1)=\frac{1}{2}\delta_\pi$.

IV. CONCLUSIONS

(a) The ground state N-Δ splitting due to pionic self-energy contribution converges satisfactorily when a realistic pion form factor is used. For the special case with no gluon splitting, the convergence is demonstrated analytically even without a pion form factor.

(b) It is misleading to include only the ground states of N and Δ as intermediate states in the pionic self-energy calculation. Inclusion of excited states reduces δ_π substantially.

(c) The final results depend very sensitively on the chosen radius of the nucleon. It is reasonable to identify this radius as the axial radius. If the gluonic hyperfine splitting δ_g is taken to be less than 200 MeV in the ground state, then the pionic self-energy gives rise to a substantial splitting in the ground state, and the experimental mass difference $(M_\Delta-M_N)$ can be reproduced.

(d) For gluonic hyperfine splitting $\delta_g\gtrsim 250$ MeV, the pionic contribution δ_π is very small and, for axial neutron radii $r_A\gtrsim 0.6$ fm, even negative. If we insist on the choice of $\alpha_\pi=0.64$ instead of 0.88 for the self-energy calculation, then for reasonable values of the axial nucleon radius no self-consistent solution is found. It may be then necessary to calculate higher-order diagrams. Note that this result comes about only if the intermediate states of higher shells ($N'\geq 1$) are included which bring a net negative contribution to δ_π.

(e) Instead of performing the involved self-energy calculations, it seems permissible to use the one-pion-exchange potential, including the δ-function part. The N-Δ splitting δ_π(OPEP) is about the same (with a realistic form factor) as in the self-energy calculation, provided $\alpha_\pi(\text{OPEP})=0.64$, in contrast with the somewhat larger value of α_π that is taken for the self-energy calculation. If the same value for α_π is taken in both approaches, then the OPEP model yields larger N-Δ splitting.

(f) No definite statement about the difference of the mean self-energies in the odd-parity excited states and the ground state could be made due to poor convergence (in both models A and B). For the excited-state calculation of the self-energy, it is not sufficient to restrict the intermediate states to the adjacent two shells. However, within the uncertainty expected from the lack of convergence, the results seem compatible with those of the OPEP model.

ACKNOWLEDGMENTS

The authors would like to thank Yuki Nogami for many helpful discussions. This work was supported by NATO Grant No. RG86/0074 for international collaboration in basic science research.

APPENDIX A: BARYON WAVE FUNCTIONS

We restrict ourselves to baryons in the u,d sector (zero strangeness). The 3-quark baryon wave function (leaving out the overall color part) is a totally symmetric product of a spin part χ^{P_S}, an isospin part ϕ^{P_T} and a spatial part $\psi_P^{N,L}(\rho,\lambda)$:

$$|B\rangle=\sum_{P,P_T,P_S}\chi^{P_S}\phi^{P_T}\psi_P^{N,L}(\rho;\lambda)f^{ST}_{PP_TP_S}\ .\tag{A1}$$

The indices P,P_S,P_T stand for the permutation symmetry, which we denote, respectively, by S, ρ, λ, and A for symmetric, mixed symmetric (ρ or λ type), and antisymmetric states with respect to exchange of quark pair. In the spatial wave functions $\psi_P^{N,L}(\boldsymbol{\rho},\boldsymbol{\lambda})$, given in detail below, $\boldsymbol{\rho}$ and $\boldsymbol{\lambda}$ are the usual intrinsic relative Jacobi coordinates

$$\boldsymbol{\rho}=\frac{1}{\sqrt{2}}(\mathbf{r}_2-\mathbf{r}_2), \quad \boldsymbol{\lambda}=\frac{1}{\sqrt{6}}(\mathbf{r}_1+\mathbf{r}_2-2\mathbf{r}_3) , \tag{A2}$$

in terms of the quark coordinates $\mathbf{r}_i$ (we have assumed the three quarks to have equal masses m_q). The spin wave functions χ^{P_S}, obtained by coupling three spin-$\frac{1}{2}$ quarks according to

$$\mathbf{s}_1+\mathbf{s}_2=\mathbf{S}_{12}, \quad \mathbf{S}_{12}+\mathbf{s}_3=\mathbf{S} , \tag{A3}$$

are, as usual, denoted by

$$\begin{aligned} \chi^s &= |[S_{12}=1,s_3=\tfrac{1}{2}]S=\tfrac{3}{2}\rangle , \\ \chi^s &= |[S_{12}=1,s_3=\tfrac{1}{2}]S=\tfrac{3}{2}\rangle , \\ \chi^\rho &= |[S_{12}=0,s_3=\tfrac{1}{2}]S=\tfrac{1}{2}\rangle . \end{aligned} \tag{A4}$$

We use the following short notation for angular momentum coupling:

$$|[J_1,J_2]JM\rangle = \sum_{\mu\mu'} \langle J_1\mu J_2\mu' | JM\rangle \, |J_1\mu\rangle \, |J_2\mu'\rangle . \tag{A5}$$

(The third component M is left out when not explicitly used.) For the Clebsch-Gordan coefficients, as well as the $3j$ and $6j$ symbols below, we use the same notation and phase convention as Edmonds.[22]

The isospin functions ϕ^s, ϕ^ρ, and ϕ^λ are completely isomorphic to the spin functions (A4), according to the couplings

$$\mathbf{t}_1+\mathbf{t}_2=\mathbf{T}_{12}, \quad \mathbf{T}_{12}+\mathbf{t}_3=\mathbf{T} . \tag{A6}$$

We then obtain six types of baryon states:

$$\begin{aligned} |\{56\}N_{11}\rangle &= \frac{1}{\sqrt{2}}(\chi^\rho\phi^\rho+\chi^\lambda\phi^\lambda)\psi_s^{N,L} , \\ |\{56\}\Delta_{33}\rangle &= \chi^s\phi^s\psi_s^{N,L} , \\ |\{70\}N^*_{11}\rangle &= \tfrac{1}{2}[(\chi^\rho\phi^\lambda+\chi^\lambda\phi^\rho)\psi_\rho^{N,L} , +(\chi^\rho\phi^\rho-\chi^\lambda\phi^\lambda)\psi_\lambda^{N,L}] , \\ |\{70\}N^*_{31}\rangle &= \frac{1}{\sqrt{2}}\chi^s(\phi^\rho\psi_\rho^{N,L}+\phi^\lambda\psi_\lambda^{N,L}) , \\ |\{70\}\Delta^*_{13}\rangle &= \frac{1}{\sqrt{2}}\phi^s(\chi^\rho\psi_\rho^{N,L}+\chi^\lambda\psi_\lambda^{N,L}) , \\ |\{20\}N^*_{11}\rangle &= \frac{1}{\sqrt{2}}(\chi^\rho\phi^\lambda-\chi^\lambda\phi^\rho)\psi_A^{N,L} . \end{aligned} \tag{A7}$$

Here the curly brackets indicate the degeneracies of the spin/flavor SU(6) multiplets of which $N_{2S+1,2T+1}$ and $\Delta_{2S+1,2T+1}$ are the nonstrange members.

In the following we shall list the spherical harmonic-oscillator wave functions $\psi_P^{N,L}(\boldsymbol{\rho},\boldsymbol{\lambda})$ which we have explicitly used in this paper. They are decomposed into product states

$$\psi_P^{N,L}(\boldsymbol{\rho},\boldsymbol{\lambda}) = \sum_{\substack{n_\rho n_\lambda \\ l_\rho l_\lambda}} [\phi_{n_\rho l_\rho}(\boldsymbol{\rho})\phi_{n_\lambda l_\lambda}(\boldsymbol{\lambda})]^L f^{P,N,L}_{n_\rho l_\rho n_\lambda l_\lambda} , \tag{A8}$$

where $[\;]^L$ indicates again the coupling of angular momenta:

$$\mathbf{l}_\rho+\mathbf{l}_\lambda=\mathbf{L} . \tag{A9}$$

L is the total intrinsic angular momentum quantum number, and N is the main oscillator quantum number

$$N=2n_\rho+l_\rho+2n_\lambda+l_\lambda=N_\rho+N_\lambda . \tag{A10}$$

In Eq. (A8), $\phi_{nl}(\mathbf{r})$ are the standard spherical harmonic-oscillator wave functions, found in any textbook, in terms of radial wave functions $R_{nl}(r)$ and spherical harmonics $Y_{lm_l}(\theta,\phi)$:

$$\phi_{nl}(\mathbf{r})=R_{nl}(r)Y_{lm_l}(\theta,\phi) \tag{A11}$$

with the normalization

$$\int_0^\infty r^2dr\, R_{n'l'}(r)R_{nl}(r)=\delta_{nn'}\delta_{ll'} . \tag{A12}$$

N=0 state. This has $L^\pi=0^+$:

$$\psi_s^{0,0}=\phi_{00}(\boldsymbol{\rho})\phi_{00}(\boldsymbol{\lambda}) . \tag{A13}$$

N=1 states. These have $L^\pi=1^-$ (2 states):

$$\psi_\lambda^{1,1}=\phi_{00}(\boldsymbol{\rho})\phi_{01}(\boldsymbol{\lambda}), \quad \psi_\rho^{1,1}=\phi_{01}(\boldsymbol{\rho})\phi_{00}(\boldsymbol{\lambda}) . \tag{A14}$$

N=2 states. These have 7 states with $L^\pi=0$, 1^+, or 2^+:

$$\begin{aligned} \psi_s^{2,0} &= -\frac{1}{\sqrt{2}}[\phi_{00}(\boldsymbol{\rho})\phi_{10}(\boldsymbol{\lambda})+\phi_{10}(\boldsymbol{\rho})\phi_{00}(\boldsymbol{\lambda})] , \\ \psi_\lambda^{2,0} &= \frac{1}{\sqrt{2}}[\phi_{00}(\boldsymbol{\rho})\phi_{10}(\boldsymbol{\lambda})-\phi_{10}(\boldsymbol{\rho})\phi_{00}(\boldsymbol{\lambda})] , \\ \psi_\rho^{2,0} &= -[\phi_{01}(\boldsymbol{\rho})\phi_{01}(\boldsymbol{\lambda})]^{L=0} , \\ \psi_\rho^{2,1} &= [\phi_{01}(\boldsymbol{\rho})\phi_{01}(\boldsymbol{\lambda})]^{L=1} , \\ \psi_s^{2,2} &= \frac{1}{\sqrt{2}}[\phi_{02}(\boldsymbol{\rho})\phi_{00}(\boldsymbol{\lambda})+\phi_{00}(\boldsymbol{\rho})\phi_{02}(\boldsymbol{\lambda})] , \\ \psi_\lambda^{2,2} &= \frac{1}{\sqrt{2}}[\phi_{02}(\boldsymbol{\rho})\phi_{00}(\boldsymbol{\lambda})-\phi_{00}(\boldsymbol{\rho})\phi_{02}(\boldsymbol{\lambda})] , \\ \psi_\rho^{2,2} &= [\phi_{02}(\boldsymbol{\rho})\phi_{02}(\boldsymbol{\lambda})]^{L=2} . \end{aligned} \tag{A15}$$

N=3 states. There are altogether 12 states with $L^\pi=1^-$, 2^-, or 3^-. We need only list the symmetric and the λ-type mixed symmetric states:

$$\begin{aligned} \psi_s^{3,3} &= \tfrac{1}{2}\{\phi_{00}(\boldsymbol{\rho})\phi_{03}(\boldsymbol{\lambda})-\sqrt{3}[\phi_{02}(\boldsymbol{\rho})\phi_{01}(\boldsymbol{\lambda})]^{L=3} , \\ \psi_s^{3,1} &= \frac{1}{\sqrt{12}}\{2[\phi_{02}(\boldsymbol{\rho})\phi_{01}(\boldsymbol{\lambda})]^{L=1} \\ &\qquad -\sqrt{3}[\phi_{00}(\boldsymbol{\rho})\phi_{11}(\boldsymbol{\lambda})]+\sqrt{5}\phi_{10}(\boldsymbol{\rho})\phi_{01}(\boldsymbol{\lambda})\} , \\ \psi_\lambda^{3,3} &= \tfrac{1}{2}\{[\phi_{02}(\boldsymbol{\rho})\phi_{01}(\boldsymbol{\lambda})]^{L=3}+\sqrt{3}\phi_{00}(\boldsymbol{\rho})\phi_{03}(\boldsymbol{\lambda})\} , \\ \psi_\lambda^{3,2} &= [\phi_{02}(\boldsymbol{\rho})\phi_{01}(\boldsymbol{\lambda})]^{L=2} , \\ \psi_{1\lambda}^{3,1} &= \frac{1}{\sqrt{8}}[\sqrt{5}\phi_{00}(\boldsymbol{\rho})\phi_{11}(\boldsymbol{\lambda})+\sqrt{3}\phi_{10}(\boldsymbol{\rho})\phi_{01}(\boldsymbol{\lambda})] , \\ \psi_{2\lambda}^{3,1} &= \frac{1}{\sqrt{24}}\{4[\phi_{02}(\boldsymbol{\rho})\phi_{01}(\boldsymbol{\lambda})]^{L=1} \\ &\qquad +\sqrt{3}\phi_{00}(\boldsymbol{\rho})\phi_{11}(\boldsymbol{\lambda})-\sqrt{5}\phi_{10}(\boldsymbol{\rho})\phi_{01}(\bar{\boldsymbol{\lambda}})\} . \end{aligned} \tag{A16}$$

The ρ-type mixed symmetric and the antisymmetric states are obtained from those in Eq. (A16) by interchanging simply the variables $\boldsymbol{\rho}$, $\boldsymbol{\lambda}$ according to the following rule:

$$\rho \leftrightarrow \lambda \, , \quad \psi_{i\rho}^{3,L} \leftrightarrow \psi_{i\lambda}^{3,L} \, , \quad \psi_{A}^{3,L} \leftrightarrow \psi_{s}^{3,L} \, . \tag{A17}$$

Note that there are two pairs of mixed-symmetric states with $L=1$; we have denoted them by $\psi_{i\lambda}^{3,1}$ and $\psi_{i\rho}^{3,1}$ with $i=1,2$. According to q (A17), we get, as an example,

$$\psi_{A}^{3,1}=\frac{1}{\sqrt{12}}\{2[\phi_{01}(\boldsymbol{\rho})\phi_{02}(\boldsymbol{\lambda})]^{L=1}-\sqrt{3}\phi_{11}(\boldsymbol{\rho})\phi_{00}(\boldsymbol{\lambda}) + \sqrt{5}\phi_{01}(\boldsymbol{\rho})\phi_{10}(\boldsymbol{\lambda})\} \, .$$

Note that the relative signs of the ρ-type and λ-type wave functions for given N and L are important. Otherwise, the overall phases are arbitrary.

APPENDIX B: CALCULATION OF MATRIX ELEMENTS

Since we work with symmetrized wave functions, we can use the rule

$$\langle B \,|\, \sum_{i=1}^{3} \hat{h}(i) \,|\, B' \rangle = 3\langle B \,|\, \hat{h}(3) \,|\, B' \rangle \tag{B1}$$

to simplify the calculation; $\hat{h}(i)$ is specified by Eqs. (2) and (3) and acts on the ith quark.

The spin and isospin parts are formally identical, so we only give as an illustration the spin matrix element which after using the Wigner-Eckardt theorem[22] becomes

TABLE III. Coefficients W_{Bi} of Eq. (B16), $i \in \{70\}$.

(a) For $B \in \{56\}$

$i \backslash B$	N_{11}	Δ_{33}
N_{11}	25	32
Δ_{33}	8	25

(b) For $B \in \{70\}$

$i \backslash B$	N_{11}^*	N_{31}^*	Δ_{13}^*
N_{11}	4	1	1
Δ_{33}	2	5	5

$$\langle [S'_{12},\tfrac{1}{2}]S'M'_s \,|\, \boldsymbol{\sigma}(3)\cdot\mathbf{k} \,|\, [S_{12},\tfrac{1}{2}]S,M_s \rangle = \delta_{S_{12},S'_{12}}(-)^{S_{12}+1/2-M'_s}\sqrt{6}\sqrt{(2S+1)(2S'+1)}\begin{Bmatrix} \frac{1}{2} & S' & S_{12} \\ S & \frac{1}{2} & 1 \end{Bmatrix} \times \sum_q \begin{pmatrix} S & S' & 1 \\ M_S & -M'_S & q \end{pmatrix} k_q \, . \tag{B2}$$

Here { } denotes the usual $6j$ symbol[22] and k_q ($q=0,\pm 1$) are the spherical-tensor components of the momentum vector $\mathbf{k}$.

The spatial matrix elements of the pion wave factor $\exp[i\mathbf{k}\cdot(\mathbf{r}_3-\mathbf{R})]=\exp(i\sqrt{2/3}\mathbf{k}\cdot\boldsymbol{\lambda})$ is obtained similarly after a partial-wave expansion:

$$\langle n'_\rho n'_\lambda(l'_\rho l'_\lambda)L'M'_L \,|\, \exp(i\sqrt{2/3}\mathbf{k}\cdot\boldsymbol{\lambda}) \,|\, n_\rho n_\lambda(l_\rho l_\lambda)LM_L \rangle = \delta_{M_L M'_L}\delta_{n_\rho n'_\rho}\delta_{l_\rho l'_\rho}[(2L+1)(2L'+1)(2l_\lambda+1)(2l'_\lambda+1)]^{1/2} \times \sum_l i^l(2l+1)\begin{pmatrix} L' & l & L \\ -M_L & 0 & M_L \end{pmatrix}\begin{pmatrix} l_\lambda & l'_\lambda & l \\ 0 & 0 & 0 \end{pmatrix}\begin{Bmatrix} l'_\lambda & L' & l_\rho \\ L & l_\lambda & l \end{Bmatrix}\langle n'_\lambda l'_\lambda \,|\, j_l(\kappa\lambda) \,|\, n_\lambda l_\lambda \rangle \, . \tag{B3}$$

Here j_l is a spherical Bessel function and $\kappa=\sqrt{2/3}k$. The radial matrix element $\langle j_l \rangle$ will be discussed below.

After squaring the matrix elements, summation over the initial states $M_S M_L$ and averaging over the intermediate states M'_S, M'_L, and T'_3, we get

$$\overline{|M_{Bi}|^2}=27\times 4\pi\alpha_\pi\frac{k^2}{m_q^2}(2T'+1)(2S'+1)(2L'+1)\sum_l G_l(2l+1) \, , \tag{B4}$$

$$G_l=\left| \sum_{\substack{l,l',S_{12},T_{12} \\ \alpha,\alpha',\beta,\beta'}} f_\beta^{ST} f_{\beta'}^{S'T'}(-)^{T_{12}+S_{12}}\begin{Bmatrix} \frac{1}{2} & T' & T_{12} \\ T & \frac{1}{2} & 1 \end{Bmatrix}\begin{Bmatrix} \frac{1}{2} & S' & S_{12} \\ S & \frac{1}{2} & 1 \end{Bmatrix} g_l^{PP'} \right|^2 \, , \tag{B5}$$

TABLE IV. Factors b_B appearing in Eq. (B16) for harmonic-oscillator states up to $N_B=3$.

	$N_B=0$	$N_B=1$		$N_B=2$		
State B	$\{56\}0^+$	$\{70\}1^-$	$\{56\}0^+$	$\{70\}0^+$	$\{56\}2^+$	$\{70\}2^+$
b_B	1	$\frac{2}{3}$	$\frac{1}{108}$	$\frac{1}{54}$	$\frac{1}{54}$	$\frac{1}{27}$
			$N_B=3$			
State B	$\{56\}1^-$	$\{56\}3^-$	$\{70\}_{1,}1^-$	$\{70\}_{2,}1^-$	$\{70\}2^-$	$\{70\}3^-$
b_B	$\frac{1}{1080}$	$\frac{1}{1620}$	$\frac{1}{216}$	$\frac{1}{1080}$	0	$\frac{1}{270}$

$$g_l^{PP'}=(-)^{l_\rho}f_\alpha^{PNL}f_{\alpha'}^{P'N'L'}[(2l_\lambda+1)(2l'_\lambda+1)]^{1/2}\begin{pmatrix} l_\lambda & l'_\lambda & l \\ 0 & 0 & 0\end{pmatrix}\begin{Bmatrix} l'_\lambda & L' & l_\rho \\ L & l_\lambda & l\end{Bmatrix}\langle n'_\lambda l'_\lambda \,|\, j_l(\kappa\lambda)\,|\, n_\lambda l_\lambda\rangle \ . \tag{B6}$$

The coefficients f_β^{ST} and f_α^{PNL} are those of Eqs. (A1) and (A8), where $\beta=(P,P_T,P_S)$ and $\alpha=(n_\rho n_\lambda l_\rho l_\lambda)$ are short notations for the quantum numbers of the initial state $|i\rangle$ and α' and β' those of the intermediate states $|B\rangle=|L',N',P',\ldots\rangle$, respectively. Note that in the $g_l^{PP'}$ only the combinations $(PP')=(S,S)$, (S,λ), (λ,λ), (ρ,ρ), (ρ,A), or (A,A) are allowed.

The above expressions simplify considerably if the initial (or the intermediate) state is a pure S state, e.g., $L=l_\rho=l_\lambda=0$ (with any n_λ,n_ρ):

$$\overline{|M_{Bi}(L=0,S,T\to L',S',T')|^2}=27.4\pi\alpha_\pi\frac{k^2}{m_q^2}(2T'+1)(2S'+1)(2L'+1)\times B_{ST,S'T'}\left|\sum_{\substack{\alpha,\alpha'\\ P,P'}}f_\alpha^{PN0}f_{\alpha'}^{P'N'L'}\langle n',L'\,|\,j_{L'}(\kappa\lambda)\,|\,n_\lambda 0\rangle\right|^2 , \tag{B7}$$

where

$$B_{ST,S'T'}=\left|\sum_{\substack{S_{12},T_{12}\\ \beta,\beta'}}f_\beta^{ST}f_{\beta'}^{S'T'}\begin{Bmatrix}\frac{1}{2} & T' & T_{12}\\ T & \frac{1}{2} & 1\end{Bmatrix}\begin{Bmatrix}\frac{1}{2} & S' & S_{12}\\ S & \frac{1}{2} & 1\end{Bmatrix}\right|^2 . \tag{B8}$$

The radial matrix element

$$\langle n'l'\,|\,j_\lambda(\kappa r)\,|\,nl\rangle=\int_0^\infty r^2dr\,R_{n'l'}(r)R_{nl}(r)j_\lambda(\kappa r) \tag{B9}$$

can be expressed, with the standard spherical harmonic-oscillator wave functions $R_{nl}(r)$, in terms of the integrals

$$F_\lambda^\mu(x)=\alpha_0^{\mu+3}\int_0^\infty r^{\mu+2}dr\,e^{-\alpha_0^2r^2}j_\lambda(\kappa r) \tag{B10}$$

with

$$x=\left[\frac{\alpha_0}{\kappa}\right]^2=\frac{3}{2}\left[\frac{\alpha_0}{k}\right]^2 ; \tag{B11}$$

α_0 is the harmonic-oscillator constant

$$\alpha_0=\sqrt{m_q\Omega} \ . \tag{B12}$$

We give the following useful formulas for the $F_\lambda^\mu(x)$:

$$F_\lambda^\lambda(x)=\frac{\sqrt{\pi}}{2^{\lambda+2}}x^{-\lambda/2}e^{-1/4x} , \tag{B13}$$

$$F_\lambda^{\mu+2}(x)=\left[\frac{\mu+3}{2}\right]F_\lambda^\mu(x)-x\frac{d}{dx}F_\lambda^\mu(x) \ . \tag{B14}$$

For the special case where the initial state is the ground state (N or Δ) with $N=0$, the averaged matrix elements take the simple form

$$\overline{|M_{Bi}|^2}=\eta_{Bi}\frac{\pi}{3}\alpha_\pi\frac{k^2}{m_q^2}e^{-k^2/3\alpha_0^2}\quad (i=N,\Delta) , \tag{B15}$$

where η_{Bi} are dimensionless constants:

$$\eta_{Bi}=W_{Bi}b_B\left[\frac{k}{\alpha_0}\right]^{2N_B} ; \tag{B16}$$

here N_B is the main oscillator constant of the intermediate state ($N_B=N'$ above). The coefficients W_{Bi} reflect the spin-isospin structure and depend only on the symmetry of the final state ($\{56\}$ or $\{70\}$), independently of N' and L'. They are given in Table III. The factors b_B depend on the individual intermediate states and are given in Table IV.

[1]A. Chodos, R. L. Jaffe, K. Johnson, and C. B. Thorn, Phys. Rev. D **10**, 2599 (1974).

[2]A. De Rújula, H. Georgi, and S. L. Glashow, Phys. Rev. D **12**, 147 (1975).

[3]N. Isgur and G. Karl, Phys. Rev. D **18**, 4187 (1978); **19**, 2653 (1979).

[4]This leads to an undesirably large value for the quark-gluon coupling constant α_s, and a correspondingly large two-body spin-orbit force. In the simplest nonrelativistic model, the hyperfine potential is taken to be of zero range, and the calculation is done in a truncated basis. The strength of α_s may be significantly reduced by taking a finite range force and doing a nonperturbative calculation, see, for example, R. K. Bhaduri, L. E. Cohler, and Y. Nogami, Phys. Rev. Lett. **44**, 1369 (1980). However, the results then depend sensitively on the chosen range of the hyperfine force, especially for a very short range.

[5]A. Chodos and C. B. Thorn, Phys. Rev. D **12**, 2733 (1975); G. E. Brown and M. Rho, Phys. Lett. **82B**, 177 (1979).

[6]S. Théberge, A. W. Thomas, and G. A. Miller, Phys. Rev. D **22**, 2838 (1980); **22**, 2106(E) (1981).

[7]A. W. Thomas, in *Advances in Nuclear Physics,* edited by J. Negele and E. Vogt (Plenum, New York, 1983), Vol. 13, p. 1; G. A. Miller, in *International Review of Nuclear Physics* edited by W. Weise (World Scientific, Singapore, 1984), Vol. 1, p. 190.

[8]Y. Nogami and N. Ohtsuka, Phys. Rev. D **26**, 261 (1982).

[9]J. Navarro and V. Vento, Nucl. Phys. **A440**, 617 (1985).

[10]M. N. V. Murthy and R. K. Bhaduri, Phys. Rev. Lett. **54**, 745 (1985); M. V. N. Murthy, M. Brack, R. K. Bhaduri, and B. K. Jennings, Z. Phys. C **29**, 385 (1985).

[11]S. A. Chin, Phys. Lett. **109B**, 161 (1982); Nucl. Phys. **A382**, 355 (1982); E. Oset, *ibid.* **A411**, 357 (1983); Y. Nogami and A. Suzuki, Prog. Theor. Phys. **69**, 1184 (1983).

[12]Y. Nogami, A. Suzuki, and N. Yamanishi, Can. J. Phys. **62**, 554 (1984).

[13]K. G. Horacsek, Y. Iwamura, and Y. Nogami, Phys. Rev. D **32**, 3001 (1985).

[14]K. L. Miller *et al.*, Phys. Rev. D **26**, 537 (1982).

[15]See, for example, J. J. Sakurai, *Advanced Quantum Mechanics* (Addison-Wesley, Reading, MA, 1967), p. 67.

[16]D. Faiman and A. W. Hendry, Phys. Rev. **173**, 1720 (1968).

[17]J. A. Niskanen, Phys. Lett. **107B**, 344 (1981).

[18]G. E. Brown and W. Weise, Phys. Rep. **22C**, 281 (1975).

[19]N. Barik and B. K. Dash, Phys. Rev. D **33**, 1925 (1986).

[20]See, for example, M. A. Preston and R. K. Bhaduri, *Structure of the Nucleus* (Addison-Wesley, Reading, MA, 1975), p. 197.

[21]S. Théberge and A. W. Thomas, Nucl. Phys. **A393**, 252 (1983).

[22]A. R. Edmonds, *Angular Momentum in Quantum Mechanics,* 2nd ed. (Princeton University Press, Princeton, NJ, 1960).